*Int. J. Electrochem. Sci.*, 13 **(2018)** 2745 – 2757, doi: 10.20964/2018.03.41

International Journal of
ELECTROCHEMICAL
SCIENCE
www.electrochemsci.org

# Degradation of Passive Film on Low-Nickel Stainless Steel in Groundwater with Different Concentration of Chloride Ions

*Xingguo Feng*[1,2,3], *Ruilong Shi*[1], *Leyuan Zhang*[1], *Yiwen Xu*[1], *Xiangying Zhang*[1], *Jing Zhang*[1], *Yunan Ding*[1], *Da Chen*[1], *Nengpan Ju*[2,*], *Xibing Zhang*[4]

[1] Jiangsu Key Laboratory of Coast Ocean Resources Development and Environment Security, College of Harbour, Coastal and Offshore Engineering, Hohai University, Nanjing 210098, Jiangsu, China
[2] State Key Laboratory of Geohazard Prevention and Geoenvironment Protection, Chengdu University of Technology, Chengdu 610059, Sichuan, China
[3] Shangdong Provincial Key Lab of Ocean Engineering, Ocean University of China, Qingdao 266100, China.
[4] Changjiang River Scientific Research Institute, Wuhan 400010, Hubei, China
[*]E-mail: jnp@cdut.edu.cn

*Received:* 16 October 2017 / *Accepted:* 3 January 2018 / *Published:* 5 February 2018

The effect of chlorides on the degradation of passivation on a low-nickel stainless steel was investigated via electrochemical testing in a simulated groundwater solution. The results revealed that, with increasing chloride concentration of the groundwater, the corrosion potential, adsorption layer resistance, and the polarization resistance of the steel decreased significantly, donor density increased, whereas the thickness of the space charge layer decreased, and pitting potential decreased significantly (as determined via potential dynamic polarization measurements). The results suggest that degradation of the passive film on the low-nickel stainless steel was considerably exacerbated by increasing chloride concentration of the groundwater.

**Keywords:** Low-nickel stainless steel; Groundwater; Mott-Schottky; Passive film; EIS.

## 1. INTRODUCTION

The long-term reliability and durability of ground anchors have attracted increased attention in recent years [1]. Owing to external environmental factors and the properties of materials, traditional ground anchors fabricated from carbon steels will undergo severe corrosion, rendering these anchors inaccessible for either inspection or renovation prior to invalidation [2]. Shaqour [3] reported that some

anchors inundated with aggressive groundwater in Kuwait City for approximately 2 years showed signs of pitting.

In extremely aggressive environments, stainless steel is more corrosion resistant than traditional carbon steel, owing to the passive film on the steel surface [4]. Alonso [5] determined the critical chloride level that induces pitting corrosion in some stainless and carbon steels. The results showed that chloride threshold values of stainless steels were at least 10 times higher than those of carbon steels. Furthermore, Medina [6] evaluated the mechanical and structural behavior of rebars, cross-sections, and structural members fabricated from stainless steels and traditional carbon steels. The findings revealed that the ductility and corrosion resistance performance of stainless steel rebars were superior to those of carbon steels. The results of these studies [4–6] suggested that stainless steels constitute acceptable alternatives to traditional carbon steels for use as ground anchors.

Though stainless steels are excellent candidates, corrosion problems will persist if the theories on the corrosion resistance of materials are neglected. Gopi [7] evaluated the pitting behavior of 304 stainless steels by using surface analytical techniques to view the anti-corrosive passive film formed on the surface of the material. The observations predicted that the steel would corrode after prolonged periods. According to a previous study [8], erosive anions, such as chlorides, sulfates, and bicarbonates in the groundwater, play an important role in inducing anchor corrosion during the service lifetime. Among these erosive anions, chlorides are particularly pervasive and have a significant influence on the passivation of stainless steels. Deanna [9] evaluated, via potential dynamic polarization curves, the electrochemical behavior of pure iron and 304L stainless steel in alcohol media with and without chloride. During the studies, chloride concentrations of up to $10^{-2}$ M induced corrosion of the stainless steel. Polarization measurements on super duplex stainless steel exposed to an electrolyte with millions of chloride ions under seven different temperatures [10] revealed that the passive films formed were slightly affected by the NaCl concentration. However, these oxide passive films underwent catalytic degradation when the temperature was increased to 60°C. Li [11] determined the influence of chlorides on the passive behavior of 316L stainless steel by evaluating the corrosion process of the material in simulated cathodic environments. Variations in the electrochemical parameters indicated that the protectiveness of the passive film increased with decreasing chloride concentrations.

However, stainless steels have yet to be fully accepted as the major material for ground anchors. From an economic point of view, stainless steels offer advantages over fully protected systems. The basic cost of stainless steel anchors is appreciably higher than that of carbon steel anchors and other costs (for example, those associated with maintenance and restoration) must also be taken into consideration [2,12]. As a result, new low-nickel stainless steel, where the nickel content (subject to considerable price undulation due to stock market factors) is partly replaced by cheaper elements, is sometimes employed. Fajardo [13] investigated the corrosion behavior of a low-nickel stainless steel in a carbonated calcium hydroxide solution where the chloride concentration was varied. This steel exhibited passive-like behavior at all concentrations, but was more prominent at higher concentrations (than at lower values). In addition, by comparing the corrosion resistance of low-nickel stainless steels and traditional AISI 304 stainless steels, the authors found that these two types of stainless steels exhibited similar corrosion behavior. Bautista [14] compared polarization test results of low-nickel 204Cu stainless steel with those of some austenitic stainless steels in simulated carbonated

and non-carbonated pore solutions, where the chloride concentration was varied. The experimental results indicated that, in extremely aggressive solutions, the corrosion resistance of 204Cu was significantly lower than that of austenitic stainless steels. Further observations in mortars confirmed that using the low-nickel 204Cu (rather than the 304 stainless steel) for structures exposed to the same environment yielded a 35%–40% reduction in the initial cost. Similarly, Monticelli [15] investigated the corrosion process of low-nickel and 304 austenitic stainless steels carbonated and exposed for 650 days to increasing amounts of chloride in alkaline-activated fly ash mortars. The findings also confirmed the excellent performance of the new low-nickel stainless steel, where the pitting resistance was only slightly lower than that of 304 stainless steel. Serdar [16] conducted long-term (i.e., 2 year) corrosion measurements via electrochemical impedance spectroscopy at the open circuit potential, on steels embedded in mortar with chloride media. The results suggested that the open circuit potential ($E_{OCP}$) of new low-nickel stainless steels approached that of traditional austenitic stainless steels, with the difference in the total resistance being small.

Previous studies have focused on the effect of chloride concentration on the corrosion resistance and pitting resistance of traditional austenitic or low-nickel stainless steel in various solutions. However, studies have rarely focused on the corrosion behavior of new low-nickel stainless steel in groundwater where the chloride content varies. In this study, the influence of chloride concentration on low-nickel stainless steel in a simulated groundwater was elucidated via open circuit potential (OCP) values, electrochemical impedance spectroscopy (EIS) measurements, Mott-Schottky plots, and potential dynamic polarization curves. These results revealed that the corrosion degree of samples in simulated groundwater increased with increasing chloride concentration. At the same time, the passive films formed on the steels were severely degraded and the space charge layers were thinned**.**

## 2. MATERIALS AND EXPERIMENTS

### *2.1 Materials*

The test specimens in this study were fabricated from low-nickel 201 stainless steel. These samples were subjected to electrochemical testing (see Figure 1 for specimen dimensions). Prior to testing, the specimens were ground with a series of emery papers down to grade 1000. After degreasing with absolute ethyl alcohol, the specimens (covered with a coating of silica gel) left a 0.5 $cm^2$ exposed area in the middle of the geometry. The concentrations of dominant erosive anions in the simulated groundwater solution (polluted with different amounts of sodium chloride, sodium sulfate, and sodium bicarbonate) were 50 times higher than those of the underground water solutions of the North Mountain in Gansu Province, China [17]. Chloride concentrations of 3 g/L, 6 g/L, 12 g/L (reference group), 24 g/L, and 48 g/L were tested (Table 1).

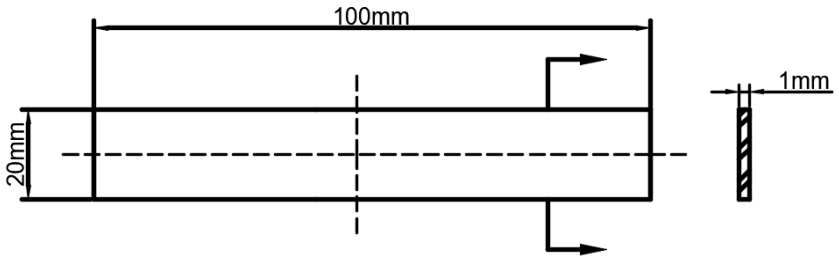


**Figure 1.** Geometry of specimens used in the simulated groundwater.

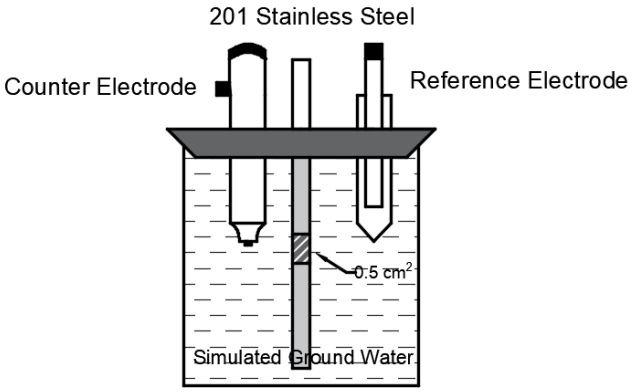


**Figure 2.** Illustration of specimen and the electrochemical test model.

**Table 1.** The concentration of ions in the simulated groundwater solution

| Solution | $Cl^-$ (g/L) | $SO_4^{2-}$ (g/L) | $HCO_3^-$ (g/L) |
|---|---|---|---|
| 1 | 3 | 11 | 1.4 |
| 2 | 6 | 11 | 1.4 |
| 3 | 12 | 11j | 1.4 |
| 4 | 24 | 11 | 1.4 |
| 5 | 48 | 11 | 1.4 |

*2.2 Experiments*

Immediately after obtaining the test specimens, electrochemical measurements were performed on the prepared samples, using the instrument shown in Figure 2. During the experiments, tests were conducted with a CS350 workstation (Corrtest Instrument, China). A traditional three-electrode cell was employed: the test specimens, a platinum plate, and a saturated calomel electrode (SCE) were used as the working, counter, and reference electrodes, respectively. Each experiment was performed in triplicate, at the same concentration, with a new sample used for each run. To remove the oxide film

formed by aerial oxidation, the specimens were all potentiostatically polarized for 5 min, at a potential of -1.0 $V_{SCE}$ prior to the experiments. After stabilizing in the simulated groundwater for 30 min, the OCP of each sample was measured for 300 s until a stable potential was reached. The OCP observed in this experiment concurred with average values calculated from the test results of three samples. During the EIS tests (a frequency range from $10^5$ to $10^{-2}$ Hz), an AC disturbance signal of 10 mV was applied to the steel electrode at the OCP. Mott-Schottky plots for evaluating the desquamation of the passive films were obtained under the following conditions: amplitude signal, 10 mV; potential step, 50 mV (from -1.5 $V_{SCE}$ to 1.5 $V_{SCE}$); and frequency, 1000 Hz [18]. In addition, potential dynamic polarization measurements were performed at a scan rate of 1 mV/s from 0.3 V below the OCP until the breakdown potential was reached (1.1 V with respect to the OCP) [10,19]. Three EIS, Mott-Schottky, and potential dynamic polarization curves were obtained for each specimen (exposed to the same chloride concentration). In each case, the middle curve was selected as the representative example that showed the influence of chloride concentration on the electrochemical behavior.

## 3. RESULTS AND DISCUSSION

### *3.1 Open circuit potential*

Figure 3 shows the OCP values of the samples monitored under different chloride concentrations. Consistent with previous studies [20], the OCP decreased significantly until the degree of chloride concentration reached a steady state value of ~200 mV below the OCP. Fajardo [20] investigated the corrosion behavior of low-nickel steel and other stainless steels in a simulated concrete pore solution where the chloride content was varied. The results indicated that the OCP decreased significantly with increasing chloride content of up to 1.0%, and changed only moderately thereafter. In the present study, the decrease in the OCP values represented severe degradation of the passive film, because of an increase in the chloride concentration.

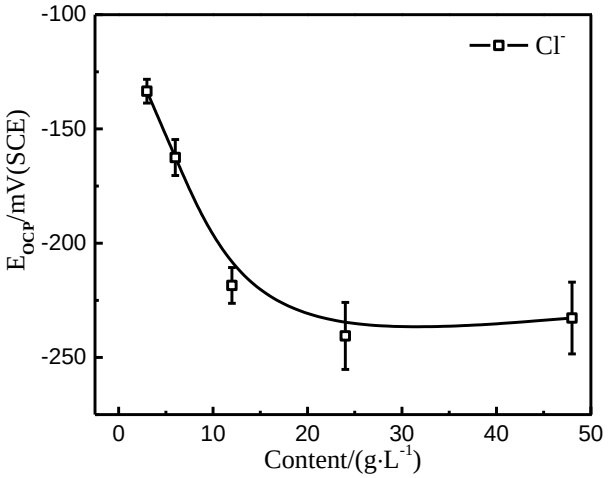


**Figure 3.** Dependence of the low-nickel stainless steel OCP on the chloride concentration of a simulated groundwater solution.

*3.2 Electrochemical impedance spectroscopy*

Figure 4a shows the Nyquist diagrams of the low-nickel 201 stainless steel immersed in simulated groundwater, where the concentration of chloride ions was varied. As the figure shows, the radius of the capacitive semi-circle decreased considerably with increasing chloride concentration. The EIS results were fitted to an equivalent circuit (Figure 5) with the help of Zsimpwin software [21,22]. As the figure shows, $R_s$ represents the resistance of the solution, while $R_{ad}$ and C are the adsorption layer resistance and capacitance, respectively. $R_p$ and Q are the polarization resistance of the corrosion process in the micropore of the passive film and the double layer capacitance [23]. The equivalent circuit yielded ideal fitting curves (see Figure 4) of the tested data. The fitting results of $R_{ad}$ and $R_p$ plotted as a function of the chloride concentration are shown in Figure 6. As the figure shows, $R_p$ and $R_{ad}$ decreased with increasing chloride concentration (i.e., the corrosion resistance of the samples decrease, owing to the dissolution of the passive film).

The $R_p$ values obtained in this study ranged from $1.08 \times 10^4$ to $2.02 \times 10^7$ $\Omega.cm^2$, and the co-domain of $R_{ad}$ ranged from 5.35 to 18.37 $\Omega.cm^2$ (i.e., the magnitude of $R_{ad}$ was lower than that of $R_p$). This difference indicated that the chloride concentration had a significant influence on $R_p$, but only a modest effect on $R_{ad}$, as reported in previous studies [24]. Using EIS methods, Li [24] investigated the effect of chloride ions on the corrosion behavior of a novel martensitic stainless steel in 0.1 M $Na_2SO_4$. The test results showed that the solution resistance and resistance of the corrosion products decreased with increasing chloride concentration, thereby resulting in dissolution of the passive films.

Variations are typical of the parameters associated with passive films. The impedance of the double layer capacitance element Q was represented by the constant phase element (CPE) rather than the pure capacitance [23,25]. The CPE impedance was calculated from:

$$Z_{CPE}=Y_0^{-1}(j\omega)^{-n} \quad (1)$$

Where, $Y_0$ was associated with the surface and electroactive properties and n represented the CPE exponent. The capacitance element $Y_0$ (CPE) corresponded to pure capacitance and pure resistance when n = 1 and n = 0, respectively. This value was also correlated with the surface heterogeneity and surface roughness [26]. Furthermore, in addition to the $R_p$, $Y_0$ was used to characterize the effect of the protective film on the stainless steel [27]. In the present experiment, equivalent circuit fitting of the EIS results yielded n values that were higher than 0.7. Each impedance depended on the film thickness, which had a positive effect on the corrosion resistance of the film (Eq. (3) and, consequently, the capacitance, $C_d$, of the double layer capacitance element Q. Therefore, $C_d$ was calculated from [28]:

$$C_d = Y_0(\omega_{MAX})^{n-1} \quad (2)$$

$$C_d = \frac{\varepsilon\varepsilon_0 S}{d} \quad (3)$$

Where, $\omega_{MAX}$ = 0.025 Hz was the frequency at which the imaginary part of the impedance (Z″) had a maximum; D was the thickness of the film; and ε and $\varepsilon_0$ were dielectric constants of the vacuum and the film, respectively. The fitted results of $Y_0$ and $C_d$ are shown in Figure 7.

The constant phase element $Y_0$ and the capacitance $C_d$ increased with increasing chloride concentration. Moreover, the fitted results of $C_d$ indicated [in accordance with Eq. (3)] that the: passive

film desquamates from the surface of the low-nickel 201 stainless steel and the thickness of the adsorbed layer decreased with increasing chloride ion concentration of the simulated groundwater solution. Experimental results obtained via EIS agreed with the data determined from the previously discussed OCP curve.

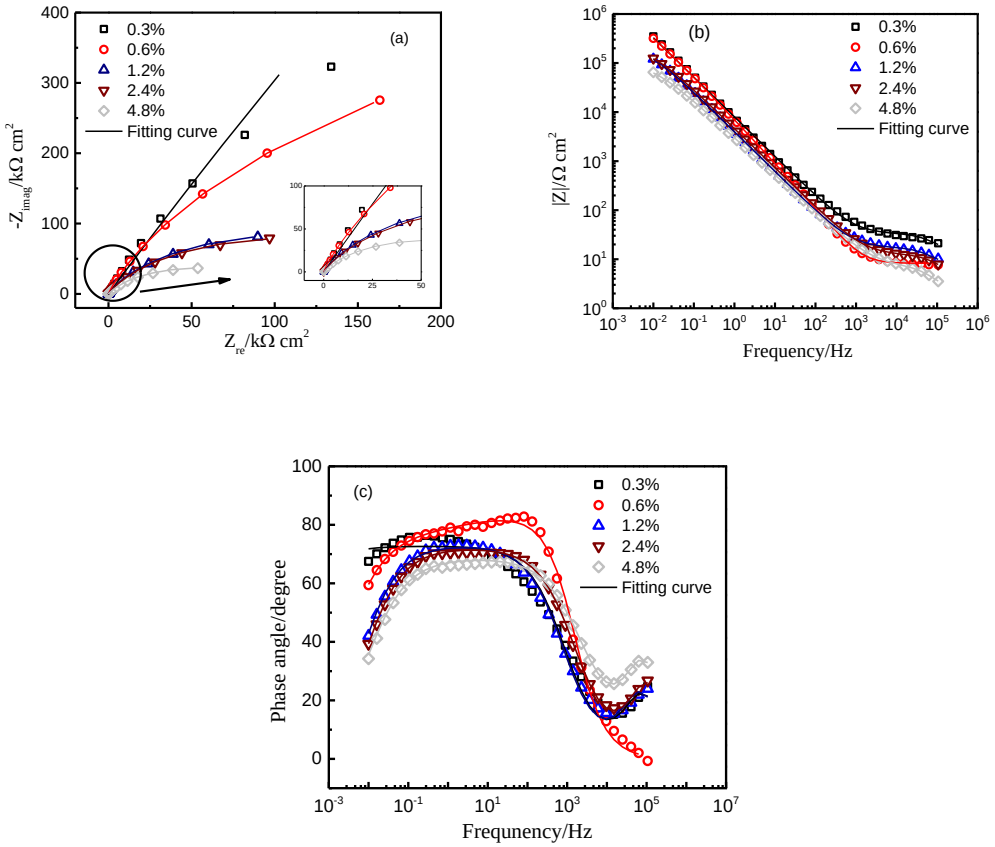


**Figure 4.** The experimental and fitted results of the low-nickel stainless steel in a simulated groundwater solution with different chloride concentrations. (a) Nyquist Plots, (b)|Z|, and (c) the phase angle.

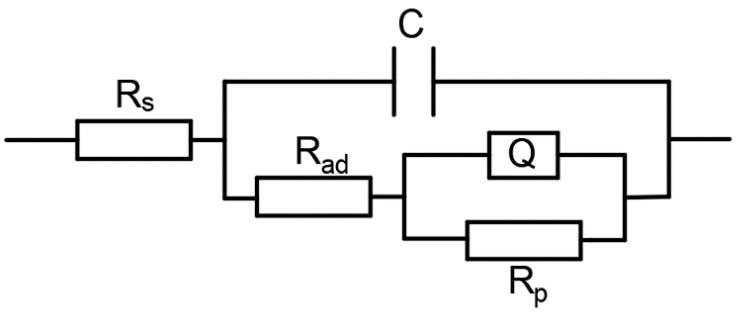


**Figure 5.** Equivalent electrical circuit used for modeling of the impedance data.

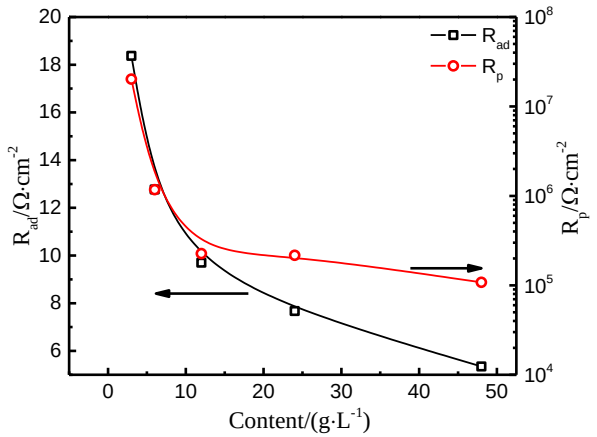


**Figure 6.** Fitting results of the adsorption layer resistance $R_{ad}$ and polarization resistance $R_p$ in a simulated groundwater solution where the chloride concentration is varied.

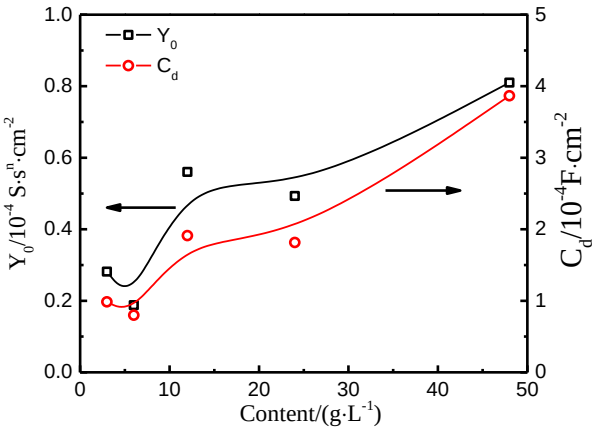


**Figure 7.** Dependence of the constant phase element $Y_0$ and space charge layer $C_d$ values on the chloride concentration of a simulated groundwater solution.

### *3.3 Semiconducting properties*

Figure 8 shows the Mott-Schottky plots of the low-nickel samples immersed in simulated groundwater where the chloride concentration was varied. The positive slopes occurring at potentials ranging from -0.5 $V_{SCE}$ to 0.2 $V_{SCE}$ suggested that the material was an n-type semiconducting film [29,30]. Taveira [30] attributed the semiconducting behavior to the passive film formed on the stainless steel, which was composed of iron oxides. Negative slopes occurred at potentials of up to 0.2 $V_{SCE}$, consistent with the initial dissolution of the passive film.

The capacitance of n-type semiconductors was calculated based on the assumption that the Helmholtz layer ($C_H$) could be neglected [31], and was as follows:

$$C^{-2} = \frac{2}{\varepsilon\varepsilon_0 q N_D}\left(E - E_{FB} - \frac{kT}{q}\right) \qquad (4)$$

where $N_D$ was the donor density of the passive film, which could be determined from the negative slope of the Mott-Schottky plots; $\varepsilon = 15.6$ [32] was the dielectric constant of the passive film;

$\varepsilon_0$ was the permittivity of free space ($8.85 \times 10^{-14}$ F/cm); q was electron charge ($1.602 \times 10^{-19}$ C); k was the Boltzmann constant; $E_{FB}$ was the flat band potential (which could be obtained by interpolating the slope to the x-axis); T was the absolute temperature, and kT/q (only about 25 mV at room temperature) was considered negligible [33]. Figure 9 shows $N_D$ plotted as a function of the chloride content. The passive film on the low-nickel stainless steel had a carrier concentration of $10^{21}$ $cm^{-3}$. The $N_D$ values plotted in Figure 9 were consistent with that ($5 \times 10^{21}$ $cm^{-3}$) reported [34] for the passive film on a high-nitrogen stainless steel surface formed in neutral NaCl solution. The $N_D$ values increased significantly and the $E_{FB}$ values (i.e., flat band potentials) became increasingly negative with increasing chloride-ion concentration of the simulated groundwater. These results indicated that, compared with lower concentrations, higher concentrations of chloride led to more severe degradation of the passive film on the low-nickel stainless steel**.**

Based on previous studies [35,36], the thickness (W) of the space charge layer could be expressed as a function of the applied potential (E) and was as follows:

$$W = [\frac{2\varepsilon\varepsilon_0}{q N_D}(E - E_{FB} - \frac{kT}{q})]^{\frac{1}{2}} \qquad (5)$$

As the W values suggested (see Figure 12), the thickness of the space charge layer decreased with increasing chloride concentration of the simulated groundwater.

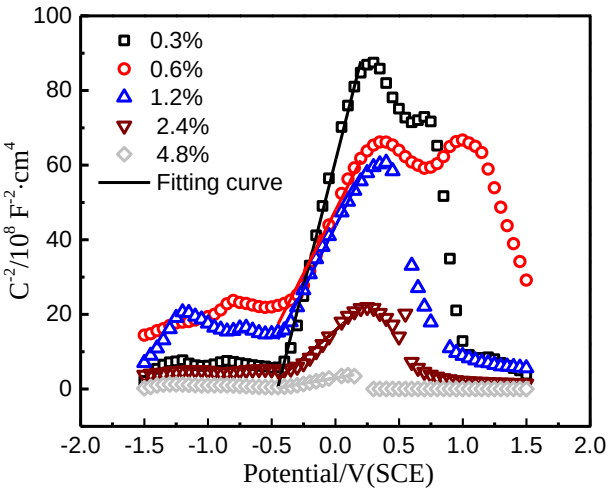


**Figure 8.** Mott-Schottky plots of the low-nickel stainless steel in a simulated groundwater solution with different chloride concentrations.

This indicated that the donor density of the passive film on the steel surface increased with thinning of the film. Therefore, the passivity of the steel decreased with increasing concentration of chloride in the simulated groundwater. Using capacitance measurements, Li [37] determined the influence of chloride ions on the electronic properties of a passive film formed on carbon steel in a $NaHCO_3/Na_2CO_3$ buffer. The results revealed that increasing concentrations of chloride ions led to accelerated corrosion of carbon steels. The author attributed this to the degradation of passive films on the steel surface (i.e., chloride ions absorbed in the film), thereby changing the composition of the film.

Consequently, the donor density of the film increased, thereby facilitating pitting corrosion of the film. These results indicated that the donor density increased with increasing concentration of chloride ions in the passive film. Therefore, compared with their susceptibility in groundwater with lower chloride concentrations, stainless steel samples were more susceptible to pitting corrosion in groundwater contaminated by higher concentrations of chloride.

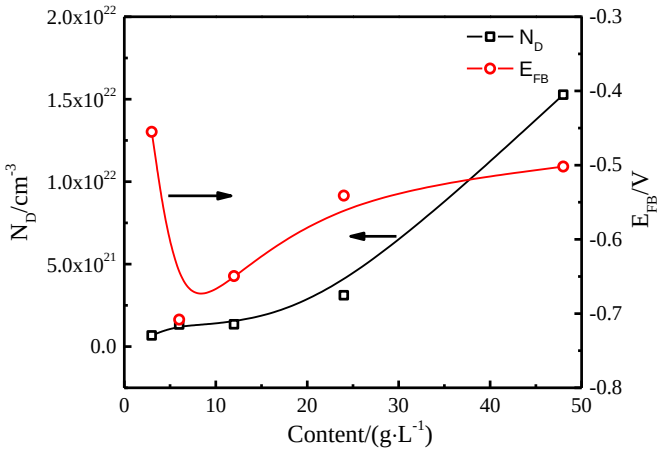


**Figure 9.** The influence of chloride concentration on the donor density and the flat band potential of passive films on the low-nickel stainless steel in a simulated groundwater solution.

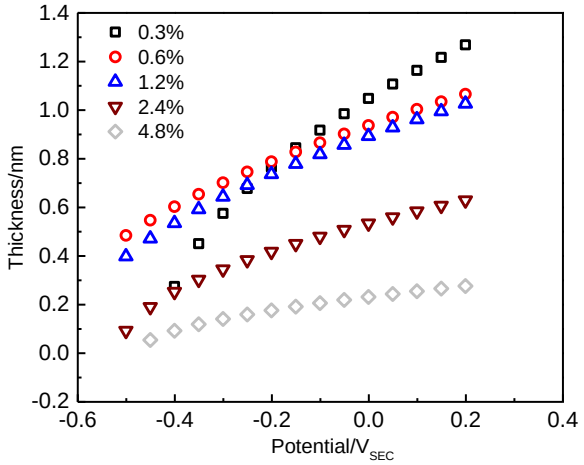


**Figure 10.** The thickness of the space charge layer on the low-nickel stainless steel in a simulated groundwater solution with different chloride concentrations.

### *3.4 Potentiodynamic polarization*

Figure 11 shows the polarization curves of the low-nickel stainless steel in the aforementioned groundwater solution (see Table 2 for the corrosion parameters determined from these curves). Among these parameters, the corrosion potential ($E_{corr}$) and current density ($i_{corr}$) were determined via the Tafel extrapolation method [38]. As Table 3 and Figure 12 show, $E_{corr}$ and $i_{corr}$ decreased and increased, respectively, with increasing concentrations of chloride ions. These trends, which are indicative of severe corrosion, agreed with the results of previous studies [22,39]. Heakal [39] compared the

influence of a systematic increase in the chloride-ion concentration on the corrosion manifestation of two types of Al-bearing TRIP steels in aqueous NaCl solutions. During potentiodynamic polarization, the parameters were dependent on the chloride concentration in solution. Increasing the molar concentration of NaCl yielded a noticeable increase in the corrosion rate with a concomitant shift of the corresponding $E_{corr}$ towards increasingly negative potentials. In the present study, the pitting potential ($E_p$) (i.e., the potential at which pitting occurred) shifts downward toward the active direction, when the chloride content was increased. This indicated that when the simulated groundwater contained a high concentration of chloride ions, passive film breakdown led to an increased likelihood of severe surface defects. The conclusions determined from the potentiodynamic polarization curves agreed with those reached on the basis of the OCP, EIS measurements, and Mott-Schottky plots. Chloride ion permeation of the passive film resulted in increased donor density and, consequently, an increase in the density of cations, which accumulated in the discontinuous area. Furthermore, several reactions inhibited the growth of the passivation film, resulting in further deterioration of the specimens. In general, high chloride ion concentrations of the simulated groundwater led to accelerated degradation of passive film**.**

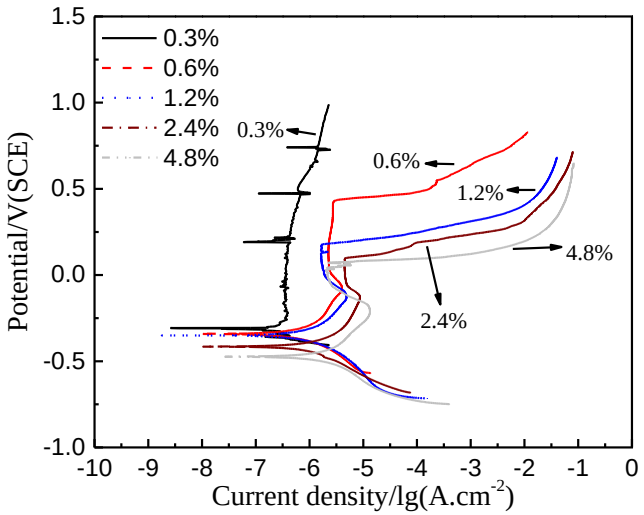


**Figure 11.** Potentiodynamic polarization curves of the low-nickel stainless steel in a simulated groundwater solution with different chloride concentrations.

**Table 2.** Corrosion parameters determined via polarization measurements of the low-nickel stainless steel in a simulated groundwater solution where the chloride concentration is varied

| Solution | $E_{corr}$ ($mV_{SCE}$) | $i_{corr}$ ($A \cdot cm^{-2}$) | $E_p$ ($mV_{SCE}$) |
|---|---|---|---|
| 1 | -307.64 | $1.664\times10^{-7}$ | —— |
| 2 | -340.83 | $2.064\times10^{-7}$ | 431.84 |
| 3 | -350.38 | $2.251\times10^{-7}$ | 176.54 |
| 4 | -415.19 | $2.992\times10^{-7}$ | 96.63 |
| 5 | -473.84 | $4.555\times10^{-7}$ | 70.16 |

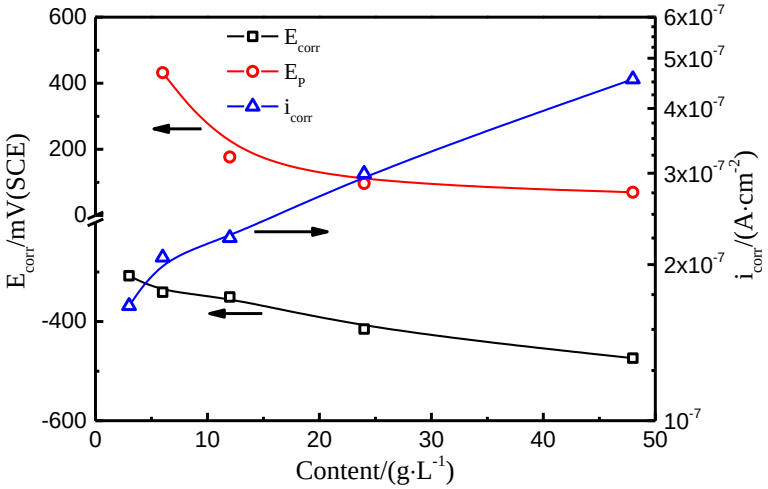


**Figure 12.** $E_{corr}$, $E_P$, and $i_{corr}$ of the low-nickel stainless steel in a simulated groundwater solution where the chloride concentration is varied.

## 4. CONCLUSIONS

Corrosion behavior of 201 low-nickel stainless steel in a simulated groundwater solution with different concentration of chloride was tested. The following conclusions can be drawn from the results:

(1) The OCP and impedance values of the low-nickel stainless steel decreased as the concentration of chloride increased. The adsorption layer resistance, $R_{ad}$, and polarization resistance, $R_p$, also significantly decreased with the content of chloride in the groundwater.

(2) The donor density, $N_D$, and flat band potential $E_{FB}$ increased with the concentration of chloride in the groundwater. Furthermore, the thickness of the space charge layer of the passive film on the low-nickel stainless steel decreased with increasing the concentration of $Cl^-$.

(3) The potentiodynamic polarization results suggested that the chloride contained in the groundwater decreased the pitting corrosion potential, and increased the current density in the anodic region for the studied steel.

ACKNOWLEDGEMENTS
The authors are grateful to the National Key R & D Program of China (no. 2017YFC0405306), the Fundamental Research Funds for the Central Universities (2015B20814), the State Key Lab of Subtropical Building Science, South China University of Technology (grant 2017ZB24), the Opening Fund of State Key Laboratory of Geohazard Prevention and Geoenvironment Protection (Chengdu University of Technology (SKLGP2017K011), the Opening Fund of Shandong Provincial Key Lab of Ocean Engineering, and the Postgraduate Research & Practice Innovation Program of Jiangsu Province (KYCX17-0451).

## References

1. Y.J. Wang, A.W. Ren, Y.S. Wang, J.Q. He and Z.Y. Chen, *Can. Geotech. J.*, 53 (2016) 589.

2. J. Mietz, J. Ruckert and B. Isecke, *Mater. Sci. Forum*., 247 (1997) 25.
3. F. Shaqour, *B. Eng. Geol. Environ.*, 65 (2006) 43.
4. L. Veleva, M.A. Alpuche-Aviles, M.K. Graves-Brook and D.O. Wipf, *J. Electroanal. Chem.*, 537 (2002) 85.
5. M.C. Garcia-Alonso, J.A. Gonzalez, J. Miranda, M.L. Escudero, M.J. Correia, M. Salta and A. Bennani, *Cement. Concrete Res.*, 37 (2007) 1562.
6. E. Medina, J.M. Medina, A. Cobo and D.M. Bastidas, *Constr. Build. Mater*., 78 (2015) 1.
7. D. Gopi, S. Manimozhi, K.M. Govindaraju, P. Manisankar and S. Rajeswari, *J. Appl. Electrochem*., 37 (2007) 439.
8. L.R. Bairi, S. Ningshen, U.K. Mudali and B. Raj, *Corros*, 68 (2012) 784.
9. P. Deanna, *Corros. Sci.*, 25 (1985) 10.
10. E.C. Souza, S.M. Rossitti and J.M.D.A. Rollo, *Mater. Charact*., 61 (2010) 240.
11. D.G. Li, J.D. Wang, D.R. Chen and P. Liang, *J. Power. Sources*., 272 (2014) 448.
12. D.V. Val, M.G. Stewart, *Struct. Saf*., 25 (2003) 343.
13. S. Fajardo, D.M. Bastidas, M.Criado and J.M. Bastidas, *Electrochim. Acta*., 129 (2014) 160.
14. A. Bautista, G. Blanco and F. Velasco, *Cement. Concrete Res.*, 36 (2006) 1922.
15. C. Monticelli, M. Criado, S. Fajardo, J.M. Bastidas, M. Abbottoni and A. Balbo, *Cement. Concrete Res.*, 55 (2014) 49.
16. M. Serdar, L.V. Zulj and D. Bjegovic, *Corros. Sci.*, 69 (2013) 149.
17. Q.F. Xu, X.L. Peng, C. Liu, *Tran. Mater. Heat. Treat.*, 20 (2015) 7. (in chinese)
18. X.G. Feng, X.Y. Lu, Y. Zuo and D. Chen, *Corros. Sci.*, 82 (2014) 347.
19. J. Izquierdo, L. Martin-Ruiz, B.M. Fernandez-Perez, R. Rodriguez-Raposo, J.J. Santana and R.M. Souto, *J. Electroanal. Chem*., 728 (2014) 148.
20. S. Fajardo, D.M. Bastidas, M. Criado, M. Romero and J.M. Bastidas, *Constr. Build. Mater*., 25 (2011) 4190.
21. C. Liu, Q. Bi, A. Leyland and A. Matthews, *Corros. Sci.*, 45 (2003) 1243.
22. S. Krakowiak, K. Darowicki and P. Slepski, *Electrochim. Acta*., 50 (2005) 2699.
23. G. Sahoo, R. Balasubramaniam, *Corros. Sci.*, 50 (2008) 131.
24. H.Y. Li, C.F. Dong, K. Xiao, X.G. Li and P. Zhong, *Int. J. Min. Met. Mater*., 23 (2016) 1286.
25. H. K, *Corros. Sci.*, 19 (1979) 11.
26. B. Cox, Y.M. Wong, *J. Nucl. Mater*., 218 (1995) 10.
27. F. Mansfeld, *Electrochim. Acta*., 35 (1990) 11.
28. C.H. Hsu, F. Mansfeld, *Corros*, 57 (2001) 747.
29. S. Faty, N. Hakiki, G. Goodlet, M.G.S. Ferreira and M.D. Belo, *Corros*, 99 (1999) 15.
30. L.V. Taveira, M.F. Montemor, M.D. Belo, M.G. Ferreira and L.F.P. Dick, *Corros. Sci.*, 52 (2010) 2813.
31. V. Vignal, M. Verneau, L. Coudreuse and R. Oltra, *Mater. Sci. Eng.*, 303 (2001) 5.
32. H.Y. Ha, M.H. Jang and T.H. Lee, *Electrochim. Acta*., 191 (2016) 864.
33. L. Hamadou, A. Kadri and N. Benbrahim, *Appl. Surf. Sci*., 252 (2005) 1510.
34. Y.X. Qiao, Y.G. Zheng, W. Ke and P.C. Okafor, *Corros. Sci.*, 51 (2009) 979.
35. U.S. Koing, *Solid. State. Ionics*., 53 (1992) 9.
36. L. Hamadou, A. Kadri and N. Benbrahim, *Corros. Sci.*, 52 (2010) 859.
37. D.G. Li, Y.R. Feng, Z.Q. Bai, J.W. Zhu and M.S. Zheng, *Electrochim. Acta*., 52 (2007) 7877.
38. F.E.T. Heakal, A.M. Fekr and M.Z. Fatayerji, *Electrochim. Acta*., 54 (2009) 1545.
39. F.E. Heakal, N.S. Tantawy and O.S. Shehta, *Mater. Chem. Phys*., 130 (2011) 743